In Situ EXAFS-Derived Mechanism of Highly Reversible Tin Phosphide/Graphite Composite Anode for Li-Ion Batteries

Yujia Ding[1*], Zhe-Fei Li[2],Elena V. Timofeeva[3], Carlo U. Segre[1]

1. Department of Physics & CSRRI, Illinois Institute of Technology;
2. Center for Electrochemical Engineering Research, Chemical and Biomolecular Engineering Department, Ohio University;
3. Department of Chemistry, Illinois Institute of Technology.

* yding12@hawk.iit.edu

Synthesis and Electrochemistry of Sn_4P_3/Graphite

$Sn_4P_3 + 9Li^+ + 9e^- \longrightarrow 4Sn + 3Li_3P$ $\quad$ $Sn + 4.4Li^+ + 4.4e^- \longleftrightarrow Li_{4.4}Sn$

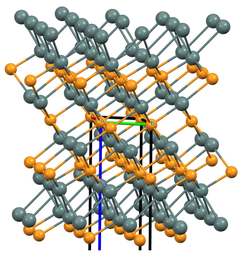

Sn_4P_3 is a promising conversion-type anode material for LIB with a theoretical capacity of 1255 mAh/g.

High energy ball milling for 6 hours under N_2

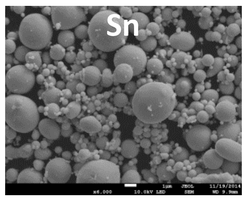

Red phosphorus

Molar ratio 4:3

Ball milling as-synthesized **Sn_4P_3** and **graphite** in a weight ratio of 7:3 for 4 hours

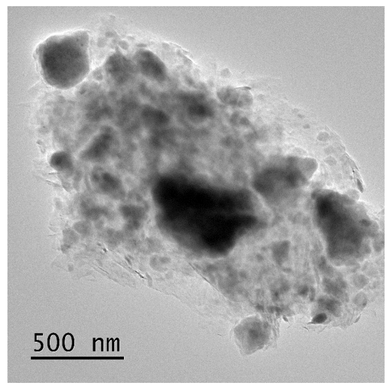

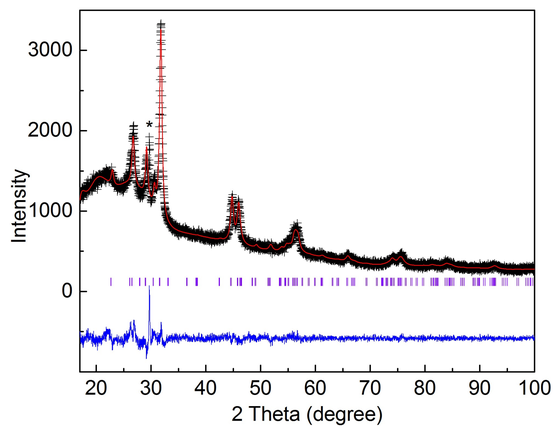

- **XRD patterns of as-synthesized Sn_4P_3/graphite composite**
- All the peaks match the Sn_4P_3 crystal structure, except the "*" peak from the mounting clay in the sample holder

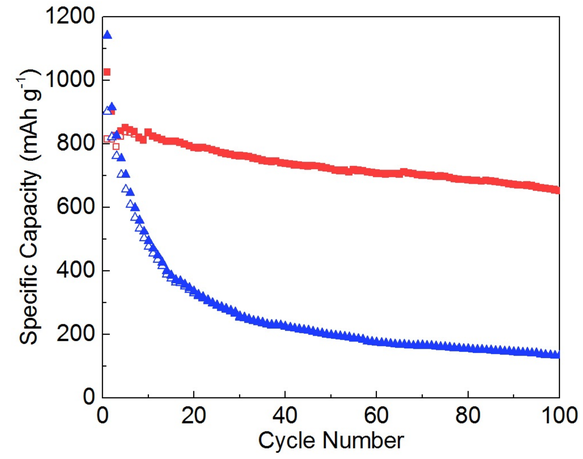

The Sn_4P_3/graphite composite (red) exhibits excellent electrochemical performance compared to pure Sn_4P_3 (blue), with a reversible capacity of 651 mAh/g in the 100th cycle.

Sn_4P_3 Electrode: 50% active materials, 10% CMC binder, 40% SuperP
Sn_4P_3/Graphite Electrode: 80% active materials, 10% CMC binder, 10% SuperP
Electrolyte: 1.2 M $LiPF_6$ in EC/EMC 3:7 with 10% FEC

In Situ EXAFS Experiment

Extended x-ray absorption fine structure (EXAFS):
Interference phenomenon between outgoing photoelectron wave and backscattered wave.

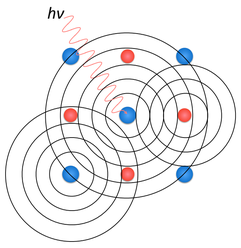

EXAFS data were collected at the Sn K-edge (29.2 keV) in fluorescence mode while the in situ coin cell was cycled galvanostatically, at MRCAT APS Sector 10-ID beamline.

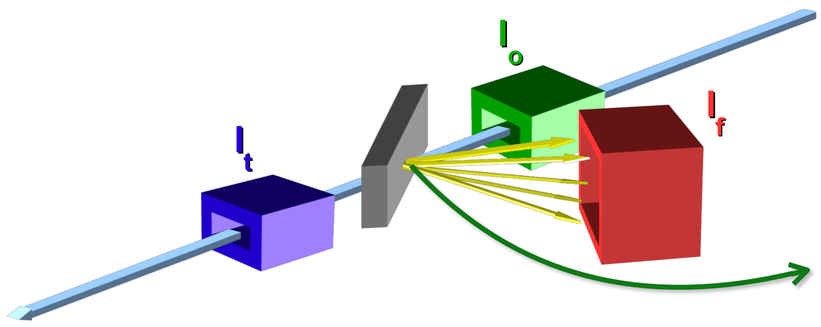

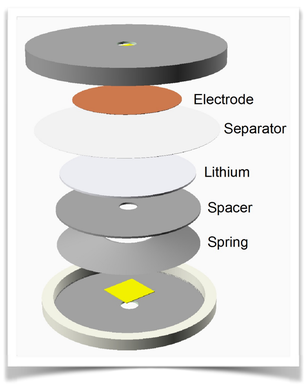

- An element-specific technique that probes the local electronic and atomic environment;
- Applicable to both crystalline and amorphous phases.
- Synchrotron x-ray can penetrate both the electrodes and the cell cases and the continuous scan methodology enables in situ study of lithiation/delithiation process.

Capacities comparison between in situ coin cell (black) and regular coin cell (red)

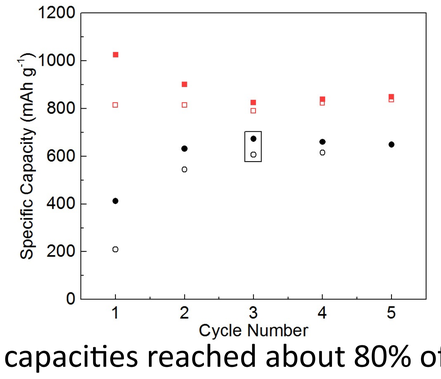

- In situ capacities reached about 80% of the regular cell in the 3rd cycle;
- Low in situ capacities are due to lower pressure and poor electrical contact in the Kapton window used for data collection.

Mechanism of Improved Cycling Performance

$|\chi(R)|$ plots of Sn_4P_3/graphite at OCV (black), lithiated (blue), and delithiated (red) states in the 3rd cycle

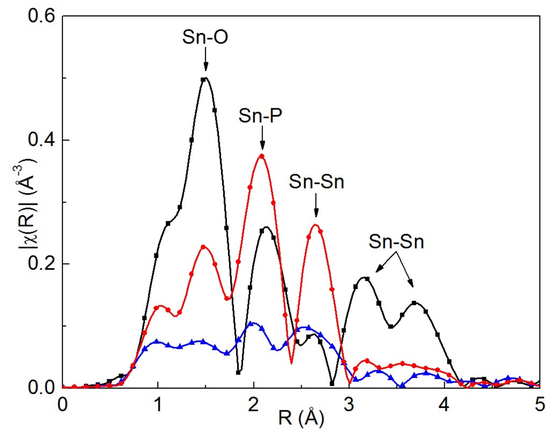

Black: Crystal structure of Sn_4P_3; High Sn-O peak is from particle surfaces or an amorphous oxide phase;
Red: Three high intensity peaks from amorphous phase; Never returns to the original crystal structure;
Blue: Low intensity peaks from LiSn alloys.

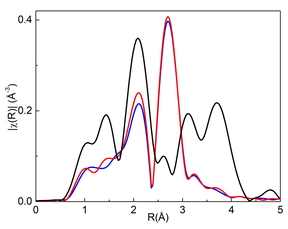

- Minor changes between the 3rd lithiated and delithiated states
- No amorphous SnP_x phase formed in pure Sn_4P_3

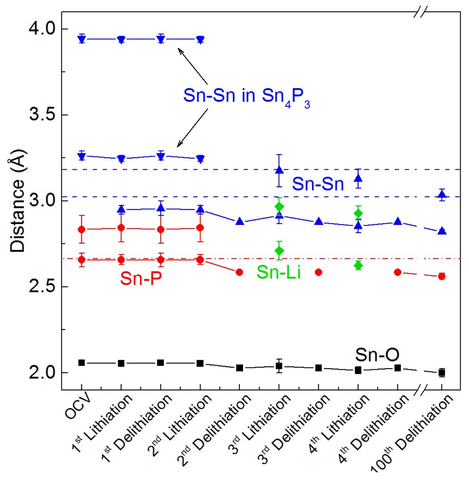

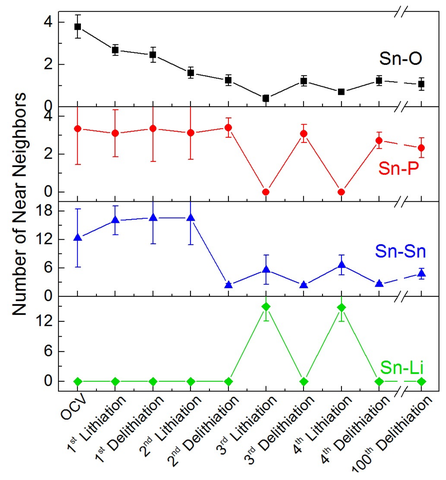

- Amorphous SnP_x phase and small metallic Sn clusters is reversibly formed in the delithiated states after the 2nd cycle, and completely decomposed in the later lithiated states. The SnP_x phase possibly exist in a tetrahedral configuration that contains only first shell P neighbors.
- The 3rd and 4th lithiated states show a mixed environment with LiSn alloys and remaining metallic Sn clusters. All Li atoms are extracted from the alloys in delithiated states.
- The gradual capacity loss after 100 cycles is due to reduced SnP_x phase and larger Sn clusters after long-term cycling.

Dynamic snapshot of $|\chi(R)|$ in the entire 3rd cycle

$SnP_x + 3xLi^+ + 3xe^- \longleftrightarrow Sn + xLi_3P$
$Sn + yLi^+ + ye^- \longleftrightarrow Li_ySn$

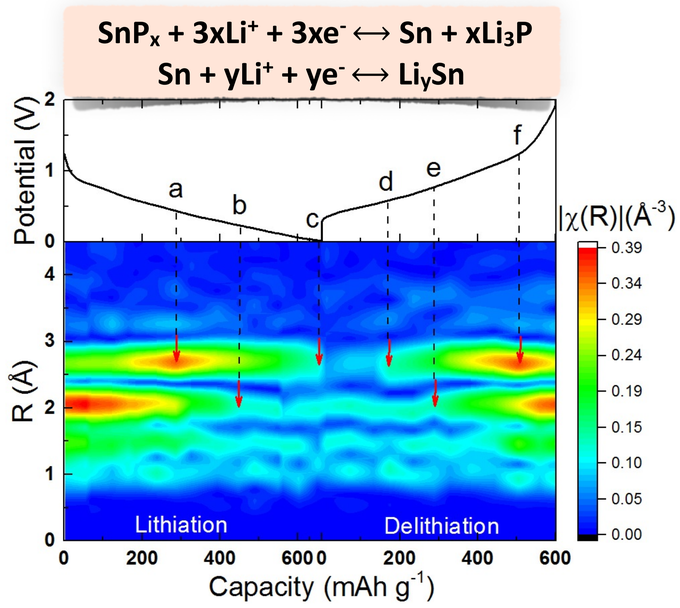

- **The formation of highly reversible amorphous SnP_x is the key to the superior capacity and cycling performance.**
- Graphite matrix enhances electrical conductivity and separates the amorphous clusters preventing aggregation during two reactions.

Acknowledgement:
This research was funded in part by U.S. Department of Energy, Advanced Research Funding Agency-Energy (ARPA-E) (Award # AR000387). MRCAT operations were supported by the Department of Energy and the MRCAT member institutions. Use of the Argonne National Laboratory Advanced Photon Source was supported by the U.S. Department of Energy, under Contract No. DE-AC02-06CH11357.

- *Adv. Energy Mater.* **2017**, 1702134